

Desoxo Molybdenum(IV) and Tungsten(IV) Bis(dithiolene) Complexes: Monomer–Dimer Interconversion Involving Reversible Thiol Bridge Formation

Amit Majumdar, Kuntal Pal, Kowliki Nagarajan, and Sabyasachi Sarkar*

Department of Chemistry, IIT Kanpur, Kanpur, India

Received April 9, 2007

Two series of thiol-bridged dimeric desoxo molybdenum(IV) and tungsten(IV) bis(dithiolene) complexes, $[\text{Et}_4\text{N}]_2\text{[M}^{\text{IV}}_2(\text{SR})_2(\text{mnt})_4]$ [$\text{M} = \text{Mo}$, $\text{R} =$ (1) $-\text{Ph}$, (2) $-\text{CH}_2\text{Ph}$, (3) $-\text{CH}_2\text{CH}_3$, (4) $-\text{CH}_2\text{CH}_2\text{OH}$; $\text{M} = \text{W}$, $\text{R} =$ (1a) $-\text{Ph}$, (2a) $-\text{CH}_2\text{Ph}$, (3a) $-\text{CH}_2\text{CH}_3$, (4a) $-\text{CH}_2\text{CH}_2\text{OH}$] and one monomeric desoxo complex, $[\text{Et}_4\text{N}]_2[\text{W}^{\text{IV}}(\text{SPh})_2(\text{mnt})_2]$ (5a) are reported. These complexes are diamagnetic, and crystal structures of each of the complex (except 5a) exhibits a dimeric $\{\text{M}^{\text{IV}}_2(\text{SR})_2\}$ core without any metal–metal bond where each metal atom possesses hexa coordination. The $\text{M}-\text{SR}$ distance ranges from 2.437 to 2.484 Å in molybdenum complexes and from 2.418 to 2.469 Å in tungsten complexes. These complexes display $\text{Mo}-\text{S}(\text{R})-\text{Mo}$ angles ranging from 92.84° to 96.20° in the case of 1–4 and $\text{W}-\text{S}(\text{R})-\text{W}$ angles ranging from 91.20° to 96.25° in the case of 1a–4a. Interestingly, both the series of Mo(IV) and W(IV) dimeric complexes respond to an unprecedented interconversion between the dimer and the corresponding hexacoordinated monomer upon change of pH. This pH-dependent interconversion establishes the fact that even the pentacoordinated Mo(IV) and W(IV) bis(dithiolene) moieties are forced to dimerize; these can easily be reverted back to the corresponding monomeric complex, reflecting the utility of dithiolene ligand in stabilizing the Mo(IV)/W(IV) moiety in synthesized complexes similar to the active sites present in native proteins.

Introduction

Monomeric molybdenum (IV) complexes are dominated by phosphorus and nitrogen donor ligands.¹ With a terminal oxo or sulfido coordination, Mo(IV) readily forms trimeric units to yield stable, $\{\text{Mo}_3\text{X}_4\}$ ($\text{X} = \text{O}, \text{S}, \text{Se}$), cuboidal clusters with molybdenum–molybdenum bonds.² The corresponding monomeric tungsten(IV) complexes are more difficult to synthesize in solution,³ and the analogous cuboidal clusters⁴ are generally made through solid-state reaction. A

rich chemistry of these clusters involving substitution of the peripheral ligands is long known.^{2c–e,5} These electron-precise cuboidal clusters were built up with the terminal chalcogen ligand stabilized $\{\text{M}^{\text{IV}}\text{X}\}$ ($\text{M} = \text{Mo}, \text{W}$; $\text{X} = \text{O}, \text{S}$) core, involving metal–metal bonds. These complexes respond to rich redox reaction⁶ and by three-electron reduction steps respond to cubane core conversion.⁷ Monomeric polychalcogenide complexes of Mo(IV)/W(IV) are unique, and their reactivity with activated acetylenes contributed a novel

* To whom correspondence should be addressed. E-mail: abyaa@iitk.ac.in.

- (1) Young, C. G. Molybdenum. In *Comprehensive Coordination Chemistry II*; McCleverty, J. A., Meyer, T. J., Wedd, A. G., Eds.; Pergamon, Elsevier: Boston, Amsterdam, 2003; Vol. 4, Chapter 4.7, pp 464–479.
- (2) (a) Shibahara, T. S. *Coord. Chem. Rev.* **1993**, *123*, 73. (b) Liao, J. H.; Li, J.; Kanatzidis, M. G. *Inorg. Chem.* **1995**, *34*, 2658–2670. (c) Raymond, C. C.; Dorhout, P. K.; Miller, S. M. *Inorg. Chem.* **1994**, *33*, 2703–2704. (d) Cotton, F. A.; Kibala, P. K.; Matusz, M.; McCaleb, C. S.; Sandor, R. B. W. *Inorg. Chem.* **1989**, *28*, 2623–2630. (e) Cotton, F. A.; Kibala, P. K.; Miertschin, C. S. *Inorg. Chem.* **1991**, *30*, 548–553. (f) Young, C. G.; Kocaba, T. O.; Yan, X. F.; Tiekink, E. R. T.; Wei, L.; Murray, H. H.; Coyle, C. L.; Stiefel, E. I. *Inorg. Chem.* **1994**, *33*, 6252–6260. (g) Yao, Y.; Akashi, H.; Sakane, G.; Shibahara, T.; Ohtaki, H. *Inorg. Chem.* **1995**, *34*, 42–48.

- (3) (a) Flomer, W. A.; Kolis, J. W. *Inorg. Chem.* **1989**, *28*, 2513–2517. (b) O’Neal, S. C.; Pennington, W. T.; Kolis, J. W. *Angew. Chem., Int. Ed. Engl.* **1990**, *29*, 1486–1488. (c) O’Neal, S. C.; Pennington, W. T.; Kolis, J. W. *Inorg. Chem.* **1992**, *31*, 888–894.
- (4) (a) Simonnet-Jegat, C.; Toscano, R. A.; Robert, F.; Daran, J. C.; Sécheresse, F. *J. Chem. Soc., Dalton Trans.* **1994**, 1311–1315. (b) Fedin, V. P.; Sokolov, M. N.; Geras’ko, O. A.; Kolesov, B. A.; Fedorov, V. Ye.; Mironov, A. V.; Yufit, D. S.; Slovohtov, Yu. L.; Struchkov, Yu. T. *Inorg. Chim. Acta* **1990**, *175*, 217–219. (c) Cotton, F. A.; Mandal, S. K. *Inorg. Chim. Acta* **1992**, *192*, 71–79. (d) Cotton, F. A.; Llusar, R.; Eagle, C. T. *J. Am. Chem. Soc.* **1989**, *111*, 4332–4338. (e) Wardle, R. W. M.; Bhaduri, S.; Chau, C. N.; Ibers, J. A. *Inorg. Chem.* **1988**, *27*, 1747–1755. (f) Bino, A.; Gibson, D. *J. Am. Chem. Soc.* **1982**, *104*, 4383–4388.
- (5) Meienberger, M. D.; Hegetschweiler, K.; Rügger, H.; Gramlich, V. *Inorg. Chim. Acta* **1993**, *213*, 157–169.

strategy to synthesize dithiolene-coordinated Mo(IV)/W(IV) complexes.⁸ These tris-chelated systems were studied extensively for their displayed geometry of trigonal pyramid over octahedral.^{3c,9} The bis-dithiolene complexes of Mo(IV) are normally stabilized with a terminal oxo coordination. Such a chromophore, {Mo^{IV}O(S₂)₂}, is important in the context of the reductase class of oxomolybdoenzymes. Thus, the Mo(IV) in the DMSO reductase family¹⁰ of molybdenum oxotransferase enzymes conserves two pterin dithiolene (S₂-pd) moieties with one terminal oxo group or the desoxo form with one protein-derived ligand, which normally varies with Ser.O⁻, Cys.S⁻, and Cys.Se⁻ residues.

Desoxo Mo/W bis(dithiolene) complexes have attracted much attention due to their close resemblance to the active site of the family of DMSO reductase. Pentacoordinated Mo/W bis(dithiolene) complexes with sterically demanding axial ligation are synthesized¹² having structural relevance to DMSOR and dissimilatory nitrate reductase^{10,11} (NiR, Chart 1). Recently, a new series of pentacoordinated monothiol-ligated Mo(IV)/W(IV) bis(dithiolene) complexes have also been reported.^{13a} The requirement of the sixth ligand for the stability of such a complex and its ready release to provide the necessary site for substrate activation have also been shown.^{13b} This synthetic approach exploited the protonation of the molybdenyl moiety present in the well-known

Chart 1. Abbreviations and designations of molybdenum and tungsten complexes.

[Et ₄ N] ₂ [Mo ^{IV} ₂ (SPh) ₂ (mnt) ₄]	1
[Et ₄ N] ₂ [Mo ^{IV} ₂ (SCH ₂ Ph) ₂ (mnt) ₄]	2
[Et ₄ N] ₂ [Mo ^{IV} ₂ (SCH ₂ CH ₃) ₂ (mnt) ₄]	3
[Et ₄ N] ₂ [Mo ^{IV} ₂ (SCH ₂ CH ₂ OH) ₂ (mnt) ₄]	4
[PPh ₄][Mo ^{IV} (SPh) ₂ (mnt) ₂]	5 ⁶
[Et ₄ N] ₂ [W ^{IV} ₂ (SPh) ₂ (mnt) ₄]	1a
[Et ₄ N] ₂ [W ^{IV} ₂ (SCH ₂ Ph) ₂ (mnt) ₄]	2a
[Et ₄ N] ₂ [W ^{IV} ₂ (SCH ₂ CH ₃) ₂ (mnt) ₄]	3a
[Et ₄ N] ₂ [W ^{IV} ₂ (SCH ₂ CH ₂ OH) ₂ (mnt) ₄]	4a
[PPh ₄][W ^{IV} (SPh) ₂ (mnt) ₂]. (CH ₃) ₂ CHOH	5a

DMSOR	dimethylsulfoxidereductase
DMSO	dimethylsulfoxide
NiR	nitrate reductase
MPT	molybdopteredithiolate
mnt	malenonitriedithiolate (2-)

complex, [Et₄N]₂[Mo^{IV}O(mnt)₂].¹⁴ It is thus interesting that in the DMSO reductase family¹⁰ of enzymes the existence of terminal oxomolybdenum(IV) and desoxo molybdenum(IV) moieties directly reflect the stability of such moieties under a specific protein fold near the active site. We have briefly reported the complex, [PPh₄][Mo^{IV}(SPh)₂(mnt)₂] (**5**), as a synthetic analogue of polysulfide reductase from *Wolinella succinogenes*¹⁵ wherein the use of an oxomolybdenum(IV) moiety was made to yield the desoxo molybdenum(IV) species. This chemistry between oxo and desoxo molybdenum(IV) moieties has now been expanded in detail in the synthesis, characterization, and reactivity of a series (Chart 1) of thiol-bridged dimeric Mo(IV) complexes: [Et₄N]₂[Mo^{IV}₂(SPh)₂(mnt)₄] (**1**), [Et₄N]₂[Mo^{IV}₂(SCH₂Ph)₂(mnt)₄] (**2**), [Et₄N]₂[Mo^{IV}₂(SCH₂CH₃)₂(mnt)₄] (**3**), and [Et₄N]₂[Mo^{IV}₂(SCH₂CH₂OH)₂(mnt)₄] (**4**). To compare the stability and reactivity pattern in parallel to the molybdenum complexes, we describe the synthesis of analogous tungsten(IV) complexes: [Et₄N]₂[W^{IV}₂(SPh)₂(mnt)₄] (**1a**), [Et₄N]₂[W^{IV}₂(SCH₂Ph)₂(mnt)₄] (**2a**), [Et₄N]₂[W^{IV}₂(SCH₂CH₃)₂(mnt)₄] (**3a**), and [Et₄N]₂[W^{IV}₂(SCH₂CH₂OH)₂(mnt)₄] (**4a**). Complex [PPh₄][W^{IV}(SPh)₂(mnt)₂] (**5a**), analogous to the molybdenum complex **5**¹⁵ has also been synthesized. All the complexes (**1–4**, **1a–5a**) are diamagnetic, as expected for this type of desoxo complexes. Interestingly, there is no metal–metal bond formation in these dimers though two units of pentacoordinated {[M^{IV}(SR)(mnt)₂]¹⁻} [M = Mo/W; R = –Ph, –CH₂CH₃, –CH₂Ph, –CH₂CH₂OH] are attached together by bridging thiolate groups. Here we generalize the pH-dependent interconversion between the dimer (**1** and **1a**) and

- (6) (a) Hong, M. C.; Li, Y.-J.; Lu, J.; Nasreldin, M.; Sykes, A. G. *J. Chem. Soc. Dalton Trans.* **1993**, 2613–2619. (b) Ghosh, M. C.; Gould, E. S. *Inorg. Chim. Acta* **1994**, 225, 297–303. (c) Tsuge, K.; Imoto, H.; Saito, T. *Inorg. Chem.* **1995**, 34, 3404–3409. (d) Li, Y. J.; Nasreldin, M.; Humanes, M.; Sykes, A. G. *Inorg. Chem.* **1992**, 31, 3011–3017. (e) Shibahara, T.; Yamasaki, M.; Sakane, G.; Minami, K.; Yabuki, T.; Ichimura, A. *Inorg. Chem.* **1992**, 31, 640–647.
- (7) (a) Sarkar, S.; Sah, R.; Chaudhury, P. K.; Maiti, R.; Das, S. K. *Proc. Indian Acad. Sci.* **1995**, 107, 355–360. (b) Weighardt, K.; Herrman, W.; Muller, A.; Eltzner, W.; Zimmermann, M. *Z. Naturforsch.* **1984**, B39, 876.
- (8) (a) Coucouvanis, D.; Hadjikyriacou, A.; Toupadakis, A.; Koo, S.-M.; Ilepurama, O.; Draganjac, M.; Salifoglou, A.; *Inorg. Chem.* **1991**, 30, 754–767. (b) Oku, H.; Ueyama, N.; Nakamura, A. *Inorg. Chem.* **1997**, 36, 1504–1516. (c) Ansari, M. A.; Mahler, C. H.; Ibers, J. A. *Inorg. Chem.* **1989**, 28, 2669–2674. (d) Lang, R. F.; Ju, T. D.; Kiss, G.; Hoff, C. D.; Bryan, J. C.; Kubas, G. J. *J. Am. Chem. Soc.* **1994**, 116, 7917–7918. (e) Formitchev, D. V.; Lim, B. S.; Holm, R. H. *Inorg. Chem.* **2001**, 40, 645–654.
- (9) (a) Garner C. D.; Charnock, J. M. Molybdenum (III), (IV) and (V). In *Comprehensive Coordination Chemistry II*; Wilkinson, G., Gillard, R. D., McCleverty, J. A., Eds.; Pergamon: Oxford, 1987; Chapter 36.4, pp 1329–1374. (b) Coucouvanis, D. *Adv. Inorg. Chem.* **1998**, 45, 1–73. (c) Wardle, R. W. M.; Mahler, C. H.; Chau, C.-N.; Ibers, J. A. *Inorg. Chem.* **1988**, 27, 2790–2795. (d) O'Neal, S. C.; Koils, J. W.; *J. Am. Chem. Soc.* **1988**, 110, 1971–1973. (e) O'Neal, S. C.; Pennington, W. T.; Kolis, J. W. *J. Am. Chem. Soc.* **1991**, 113, 710–712. (f) Young, C. G.; McInerney, I. P.; Bruck, M. A.; Enemark, J. H. *Inorg. Chem.* **1990**, 29, 412–416.
- (10) Hille, R. *Chem. Rev.* **1996**, 96, 2757–2816. (b) Hille, R. *Trends Biochem. Sci.* **2002**, 27, 360–367.
- (11) Dias, J. M.; Than, M. E.; Humm, A.; Huber, R.; Bourenkov, G. P.; Bartunik, H. D.; Bursakov, S.; Calvete, J.; Caldeira, C.; Carneiro, J. J.; Moura, G.; Moura, I.; Ramao, M. J. *Structure* **1999**, 7, 65–79.
- (12) (a) Lim, B. S.; Holm, R. H. *J. Am. Chem. Soc.* **2001**, 123, 1920–1930. (b) Sung, K.-M.; Holm, R. H. *J. Am. Chem. Soc.* **2001**, 123, 1931–1943. (c) Lim, B. S.; Donahue, J. P.; Holm, R. H. *Inorg. Chem.* **2000**, 39, 263–273. (d) Lim, B. S.; Sung, K.-M.; Holm, R. H. *J. Am. Chem. Soc.* **2000**, 122, 7410–7411. (e) Jiang, J.; Holm, R. H. *Inorg. Chem.* **2004**, 43, 1302–1310. (f) Sung, K.-M.; Holm, R. H. *Inorg. Chem.* **2000**, 39, 1275–1281.
- (13) (a) Jiang, J.; Holm, R. H. *Inorg. Chem.* **2005**, 44, 1068–1074. (b) Majumdar, A.; Pal, K.; Sarkar, S. *J. Am. Chem. Soc.* **2006**, 128, 4196–4197.

- (14) (a) Das, S. K.; Chaudhury, P. K.; Biswas, D.; Sarkar, S. *J. Am. Chem. Soc.* **1994**, 116, 9061–9070. (b) Maity, R.; Nagarajan, K.; Sarkar, S. *J. Mol. Struct.* **2003**, 656, 169–176.
- (15) Nagarajan, K.; Joshi, H. K.; Chaudhuri, P. K.; Pal, K.; Cooney, J. A.; Enemark, J. H.; Sarkar, S. *Inorg. Chem.* **2004**, 43, 4532–4533.

the corresponding monomer (**5** and **5a**). In basic pH and in the presence of excess thiolate ion, the dimeric complexes are converted to the monomeric ones, whereas the monomeric species are converted to the dimeric ones in acidic pH. Such interchange may have relevance to the variation in the active-site structure under the influence of varied apoprotein environments in the native proteins. Dimerization of the reactive pentacoordinated Mo(IV)/W(IV) bis(dithiolene) complexes, $\{[M^{IV}(SR)(mnt)_2]^{1-}\}$ [$R = -Ph, -CH_2-CH_3, -CH_2Ph, -CH_2CH_2OH$] without the formation of metal–metal bond and the facile pH-dependent interconversion of these dimers to the corresponding monomeric desoxo complexes described herein not only showed the way to synthesize such desoxo complexes which can functionally mimic^{13b} the active site of nitrate reductase but also demonstrates the utility of the dithiolene moiety in stabilizing the Mo(IV) state in synthesized desoxo complexes, as well as in the native oxidoreductase class of molybdoenzymes.

Experimental Section

Materials and Methods. All reactions and manipulations were performed under pure argon atmosphere using modified Schlenk techniques. PhSH, CH₃CH₂SH, PhCH₂SH, and OHCH₂CH₂SH were obtained from Lancaster. PPh₄Br was obtained from Alfa-Aesar. [Et₄N][Br], Et₃N, and CH₃SO₃H were obtained from S. D. Fine Chemicals Ltd., India. Solvents were dried and distilled by standard procedures. [Et₄N]₂[Mo^{IV}O(mnt)₂],¹⁴ [Et₄N]₂[W^{IV}O(mnt)₂],¹⁶ and [PPh₄][Mo^{IV}(SPh)₂(mnt)₂]¹⁵ were prepared following the process reported earlier. Infrared spectra were recorded on a Bruker Vertex 70, FT-IR spectrophotometer as pressed KBr disks. Elemental analyses for carbon, hydrogen, nitrogen, and sulfur were recorded with Perkin-Elmer 2400 microanalyzer. Electronic spectra were recorded on USB 2000 (Ocean Optics Inc.) UV–visible spectrophotometer equipped with fiber optics and on a Cintra 10 UV–visible spectrophotometer. Mass spectra (negative ion) were recorded on a Micromass Quattro II triple quadrupole mass spectrometer with an analytical electrospray source. The ESI capillary was set at 3.5 kV, and the cone voltage was 40 V. The spectra were collected in 6 s scans. Cyclic voltammetric measurements were made with BASi Epsilon, EC Bioanalytical Systems, Inc. Cyclic voltammograms and differential pulse polarographs of 10⁻³ M solution of the compounds were recorded with glassy carbon electrode as working electrode with 0.2 M Bu₄NClO₄ as supporting electrolyte, Ag/AgCl electrode as reference electrode, and platinum auxiliary electrode. Sample solutions were prepared in dichloromethane or in acetonitrile (in the case of **4** and **4a**). All electrochemical experiments were done under argon atmosphere at 298 K. Potentials are referenced against internal ferrocene (Fc) and are reported relative to the Ag/AgCl electrode ($E_{1/2}(Fc^+/Fc) = 0.459$ V vs Ag/AgCl electrode). Magnetic susceptibility measurements were carried out by using an EV7 vibrating sample magnetometer. Solution instability of the complexes in the small time range thwarted our attempts to use NMR spectroscopy.

Synthesis. [Et₄N]₂[Mo^{IV}₂(SPh)₂(mnt)₄] (**1**). [Et₄N]₂[Mo^{IV}O(mnt)₂] (4 mmol, 2.61 g) was dissolved in 50 mL of dichloromethane along with 16 mmol (1.7 mL) of thiophenol. To this green-colored solution at 0 °C, 0.5 mL of methanesulfonic acid was added dropwise with constant stirring to get a deep violet-

colored solution. Stirring was continued for 30 min at 0 °C. An oily mass was separated upon addition of 150 mL of petroleum ether (60–80 °C) into the reaction solution, which was thoroughly washed with isopropanol followed by diethyl ether to leave out a microcrystalline violet solid. This solid was recrystallized from acetonitrile; isopropanol and diethyl ether in the presence of a trace amount of thiophenol to produce violet-colored bright square block-type diffraction-quality crystals. Yield 85% (2.09 g). Anal. Calcd for Mo₂S₁₀C₄₄N₁₀H₅₀: C, 42.91; H, 4.09; N, 11.37; S, 26.038. Found: C, 43.05; H, 4.15; N, 11.45; S 26.10. Absorption spectrum (dichloromethane) λ_{max} (ϵ_M): 379 (11 242), 522 (6368), 579 (6332), 750 (sh, 1501) nm. IR (KBr pellet): ν 1475 (C=C), 2206 (CN), 3055 (aromatic CH stretching), 737 (aromatic CH bending) cm⁻¹. ESMS: $m/z = 1102$ indicative of [Et₄N][Mo^{IV}₂(SPh)₂(mnt)₄]¹⁻.

[Et₄N]₂[Mo^{IV}₂(SCH₂Ph)₂(mnt)₄] (**2**). A procedure similar to that used in the synthesis of **1** was followed to obtain a pink solid. This solid was recrystallized from dichloromethane and petroleum ether (60–80 °C) in the presence of trace amount of PhCH₂SH to yield dark pink-colored square block-type diffraction-quality crystals. Yield: 85% (2.17 g). Anal. Calcd for Mo₂S₁₀C₄₆N₁₀H₅₄: C, 43.86; H, 4.32; N, 11.12; S, 25.41. Found: C, 43.52; H, 4.63; N, 11.23; S, 25.11. Absorption spectrum (dichloromethane) λ_{max} (ϵ_M): 379 (11 387), 443 (sh, 5955), 516 (7532), 565 (6476), 750 (sh, 1235) nm. IR (KBr pellet): ν 1481 (C=C), 2206 (CN), 3050 (aromatic CH stretching), 699 (aromatic CH bending) cm⁻¹. ESMS: $m/z = 1130$ indicative of [Et₄N][Mo^{IV}₂(SCH₂Ph)₂(mnt)₄]¹⁻.

[Et₄N]₂[Mo^{IV}₂(SCH₂CH₃)₂(mnt)₄] (**3**). A procedure similar to that used in the synthesis of **1** was followed to obtain a pink solid. This solid was recrystallized from dichloromethane and petroleum ether (60–80 °C) in the presence of trace amount of CH₃CH₂SH to obtain bright pink block-shaped diffraction-quality single crystals. Yield: 85% (1.93 g). Anal. Calcd for Mo₂S₁₀C₃₆N₁₀H₅₀: C, 38.08; H, 4.44; N, 12.24; S, 28.24. Found: C, 38.43; H, 4.75; N, 12.81; S, 28.64. Absorption spectrum (dichloromethane) λ_{max} (ϵ_M): 379 (10 275), 444 (sh, 5594), 516 (7006), 565 (sh, 5498), 750 (sh, 1213) nm. IR (KBr pellet): ν 1481 (C=C), 2206 (CN) cm⁻¹. ESMS = 1006 indicative of [Et₄N][Mo^{IV}₂(SCH₂CH₃)₂(mnt)₄]¹⁻.

[Et₄N]₂[Mo^{IV}₂(SCH₂CH₂OH)₂(mnt)₄] (**4**). A procedure similar to that used in the synthesis of **1** was followed to obtain a reddish-pink-colored oily mass. This oily mass was dissolved in acetonitrile into which addition of isopropanol and diethyl ether in the presence of a trace amount of OHCH₂CH₂SH yielded bright reddish-pink-colored needle-shaped diffraction-quality crystals. Yield: 85% (1.98 gm). Anal. Calcd for Mo₂S₁₀C₃₆N₁₀H₅₀O₂: C, 37.04; H, 4.32; N, 12.00; S, 27.47. Found: C, 37.45; H, 4.74; N, 12.24; S, 27.86. Absorption spectrum (acetonitrile) λ_{max} (ϵ_M): 379 (12 066), 442 (sh, 6600), 516 (8351), 565 (sh, 6897), 750 (sh, 1369) nm. IR (KBR pellet): ν 3500 (O–H) 1486 (C=C), 2206 (CN) cm⁻¹. ESMS: $m/z = 1038$ indicative of [Et₄N][Mo^{IV}₂(SCH₂CH₂OH)₂(mnt)₄]¹⁻.

[Et₄N]₂[W^{IV}₂(SPh)₂(mnt)₄] (**1a**). [Et₄N]₂[W^{IV}O(mnt)₂] (4 mmol, 2.96 g) was dissolved in 50 mL of dichloromethane along with 16 mmol (1.7 mL) of thiophenol. To this green-colored solution at 0 °C, 0.5 mL of methanesulfonic acid was added dropwise with constant stirring to get a red-colored solution. Stirring was continued for 30 min at 0 °C. A red-colored oily mass was separated upon addition of petroleum ether (60–80 °C) into the reaction solution and on standing at 0 °C. This oily mass was dissolved in acetonitrile into which addition of isopropanol and diethyl ether in the presence of a trace amount of PhCH₂SH yielded red-colored needle-shaped diffraction-quality crystals. Yield: 85% (2.39 gm). Anal. Calcd for W₂S₁₀C₄₄H₅₀N₁₀: C, 37.55; H, 3.58; N, 9.95; S, 22.78. Found: C, 37.68; H, 3.72; N, 9.86; S, 22.92. Absorption spectrum (dichloromethane) λ_{max} (ϵ_M): 452 (7824), 535 (sh, 4726), 670 (sh, 1305).

(16) Das, S. K.; Biswas, D.; Maiti, R.; Sarkar, S. *J. Am. Chem. Soc.* **1996**, *118*, 1387–1397.

IR (KBr pellet): ν 1475 (C=C), 2204 (CN), 3055 (aromatic CH stretching), 737 (aromatic CH bending) cm^{-1} . ESMS: $m/z = 1276$ indicative of $[\text{Et}_4\text{N}][\text{W}^{\text{IV}}_2(\text{SPh})_2(\text{mnt})_4]^{1-}$.

$[\text{Et}_4\text{N}]_2[\text{W}^{\text{IV}}_2(\text{SCH}_2\text{Ph})_2(\text{mnt})_4]$ (2a). A procedure similar to that used in the synthesis of **1a** was followed to obtain a red-colored oily mass. This oily mass was dissolved in acetonitrile into which addition of isopropanol and diethyl ether in the presence of a trace amount of PhCH_2SH yielded red-colored needle-shaped diffraction-quality crystals. Yield: 85% (2.44 gm). Anal. Calcd for $\text{W}_2\text{S}_{10}\text{C}_{46}\text{H}_{54}\text{N}_{10}$: C, 38.49; H, 3.79; N, 9.75; S, 22.34. Found: C, 38.56; H, 3.72; N, 9.86; S, 22.40. Absorption spectrum (dichloromethane) λ_{max} (ϵ_{M}): 422 (11 330), 525 (sh, 5616), 670 (sh, 1572). IR (KBr pellet): ν 1482 (C=C), 2204 (CN), 3050 (aromatic CH stretching), 699 (aromatic CH bending) cm^{-1} . ESMS: $m/z = 1306$ indicative of $[\text{Et}_4\text{N}][\text{W}^{\text{IV}}_2(\text{SCH}_2\text{Ph})_2(\text{mnt})_4]^{1-}$.

$[\text{Et}_4\text{N}]_2[\text{W}^{\text{IV}}_2(\text{SCH}_2\text{CH}_3)_2(\text{mnt})_4]$ (3a). A procedure similar to that used in the synthesis of **1a** was followed to obtain a red-colored oily mass. This oily mass was dissolved in acetonitrile into which addition of isopropanol and diethyl ether in the presence of a trace amount of $\text{CH}_3\text{CH}_2\text{SH}$ yielded red-colored needle-shaped diffraction-quality crystals. Yield: 85% (2.23 gm). Anal. Calcd for $\text{W}_2\text{S}_{10}\text{C}_{36}\text{H}_{50}\text{N}_{10}\text{O}_2$: C, 37.98; H, 3.84; N, 10.68; S, 24.45. Found: C, 38.08; H, 3.92; N, 10.75; S, 24.51. Absorption spectrum (dichloromethane) λ_{max} (ϵ_{M}): 416 (13 984), 525 (sh, 5800), 670 (sh, 1744). IR (KBr pellet): ν 1482 (C=C), 2204 (CN) cm^{-1} . ESMS: $m/z = 1180$ indicative of $[\text{Et}_4\text{N}][\text{W}^{\text{IV}}_2(\text{SCH}_2\text{CH}_3)_2(\text{mnt})_4]^{1-}$.

$[\text{Et}_4\text{N}]_2[\text{W}^{\text{IV}}_2(\text{SCH}_2\text{CH}_2\text{OH})_2(\text{mnt})_4]$ (4a). A procedure similar to that used in the synthesis of **1a** was followed to obtain a red-colored oily mass. This oily mass was dissolved in acetonitrile into which addition of isopropanol and diethyl ether in the presence of a trace amount of $\text{OHCH}_2\text{CH}_2\text{SH}$ yielded red-colored needle-shaped diffraction-quality crystals. Yield: 85% (2.28 gm). Anal. Calcd for $\text{W}_2\text{S}_{10}\text{C}_{36}\text{H}_{50}\text{N}_{10}\text{O}_2$: C, 32.19; H, 3.75; N, 10.43; S, 23.87. Found: C, 32.24; H, 3.79; N, 10.48; S, 23.91. Absorption spectrum (acetonitrile) λ_{max} (ϵ_{M}): 416 (14 418), 525 (sh, 5365), 670 (sh, 1310). IR (KBr pellet): ν 3500 (O-H), 1486 (C=C), 2206 (CN) cm^{-1} . ESMS: $m/z = 1212$ indicative of $[\text{Et}_4\text{N}][\text{W}^{\text{IV}}_2(\text{SCH}_2\text{CH}_2\text{OH})_2(\text{mnt})_4]^{1-}$.

$[\text{Ph}_4\text{P}]_2[\text{W}^{\text{IV}}(\text{SPh})_2(\text{mnt})_2] \cdot 0.5\{(\text{CH}_3)_2\text{CHOH}\}$ (5a). $[\text{Et}_4\text{N}]_2[\text{W}^{\text{IV}}\text{O}(\text{mnt})_2]$ (4 mmol, 2.96 g) and 8 mmol (3.36 g) of tetraphenyl phosphonium bromide were dissolved in 50 mL of chloroform, and 40 mmol (4.25 mL) of thiophenol was added to it at 0 °C. Upon addition of 4 mmol (0.8 g) of phosphorus pentachloride, the initial purple color of the solution changed to brown. Addition of 4 mL of triethylamine followed by petroleum ether (60–80 °C) yielded a brown-colored oily compound. This was dissolved in acetonitrile into which addition of isopropanol and diethyl ether yielded brown-colored needle-shaped diffraction-quality crystals. Yield: 70% (3.89 gm). Anal. Calcd for $\text{W}_2\text{S}_6\text{C}_{68}\text{H}_{50}\text{N}_4\text{P}_2 \cdot 0.5\{(\text{CH}_3)_2\text{CHOH}\}$: C, 59.99; H, 3.91; N, 4.02; S, 13.83. Found: C, 59.85; H, 3.88; N, 4.09; S, 13.79. Absorption spectrum (dichloromethane) λ_{max} (ϵ_{M}): 380 (10 280), 440 (7850), 486 (sh, 5873), 555 (sh, 2062), 704 (sh, 581). IR (KBr pellet): ν 1482 (C=C), 2194 (CN), 3055 (aromatic CH stretching), 722 (aromatic CH bending) cm^{-1} . ESMS: $m/z = 1023$ indicative of $[\text{PPh}_4][\text{W}^{\text{IV}}_2(\text{SPh})_2(\text{mnt})_4]^{1-}$.

X-ray Crystallography. Suitable diffraction-quality single crystals were obtained from the crystallization procedures described in each synthesis. The crystals used in the analyses were glued to glass fibers and mounted on a BRUKER SMART APEX diffractometer. The instrument was equipped with a CCD area detector, and data were collected using graphite-monochromated Mo K α radiation ($\lambda = 0.71069$ Å) at low temperature (100 K). Cell constants were obtained from the least-squares refinement of three-

dimensional centroids through the use of CCD recording of narrow ω rotation frames, completing almost all-reciprocal space in the stated θ range. All data were collected with SMART 5.628 (BRUKER, 2003), and were integrated with the BRUKER SAINT program. The structure was solved using SIR97¹⁷ and refined using SHELXL-97.¹⁸ Crystal structures were viewed using ORTEP.¹⁹ The space group of the compounds was determined on the basis of the lack of systematic absence and intensity statistics. Full-matrix least-squares/difference Fourier cycles were performed which located the remaining non-hydrogen atoms. All non-hydrogen atoms were refined with anisotropic displacement parameters. Each complex (**1**, **3**, **4**, **1a**, **2a**, **3a**, **4a**, **5a**) possesses only one molecule in their respective asymmetric unit. In the asymmetric unit of compound **2**, there are three independent Mo-dimeric units of which one (Mo1–Mo2) is structurally discussed with its ORTEP plot (Figure 1b). The additional symmetry for **2** has been checked through PLATON. Single crystals of complex **2** were grown from three different batches, but all these possess similar crystallographic asymmetric units. Each ethyl group of one of the tetraethylammonium cations in **1**, **2**, and **4** is disordered over two positions. In **2**, the phenyl ring (C47–C52) of benzylthiolato group is disordered over two positions. All these disordered positions were refined using free variables (PART). The structures of **2a** suffered from disordered and unidentified solvent (CH_3CN /isopropanol/diethyl ether) in the lattice, which was not included in the refinement but was taken care of by the SQUEEZE procedure (from PLATON). The volumes occupied by the solvent were 1049.5, 1115.6, and 214.4 Å³, respectively; the number of electrons per unit cell deduced by SQUEEZE were 301.5, 12, and 12. The details of SQUEEZE results were appended to the crystallographic data file.

Results and Discussions

Synthesis. The synthetic strategy adopted here is originated from the earlier observation¹⁶ that acidified $[\text{Et}_4\text{N}]_2[\text{W}^{\text{IV}}\text{O}(\text{mnt})_2]$ ¹⁶ is converted to the corresponding tris $[\text{Et}_4\text{N}]_2[\text{W}^{\text{IV}}(\text{mnt})_3]$ ^{20,12c} complex in 60% yield. However, the same reaction in the presence of 1 equiv of Na_2mnt led to the isolation of tris $[\text{Et}_4\text{N}]_2[\text{W}^{\text{IV}}(\text{mnt})_3]$ in 90% yield. The chemistry of such a reaction can readily be interpreted as the aquation of the $\{\text{W}=\text{O}\}$ group under acidic condition to yield the $\{\text{W}(\text{OH})_2\}$ moiety in forming unstable $[\text{Et}_4\text{N}]_2\{\text{W}^{\text{IV}}(\text{OH})_2(\text{mnt})_2\}$ species which rearranged to yield the stable tris species in almost quantitative yield (67%). This reaction is substantiated on adding 1 equiv of Na_2mnt in the reaction mixture which provided the stoichiometric rest third of the ligand to raise the yield of the isolable product to 90%. It is

- (17) Altomare, A.; Burla, M. C.; Camalli, M.; Cascarano, G. L.; Giacovazzo, C.; Guagliardi, A.; Moliterni, A. G. G.; Polidori, G.; Spagna, R. *J. Appl. Crystallogr.* **1999**, *32*, 115–119.
 (18) Sheldrick, G. M. *SHELX97, Programs for Crystal Structure Analysis (Release 97-2)*; University of Göttingen: Göttingen, Germany, 1997.
 (19) Farrugia, L. J. *J. Appl. Crystallogr.* **1997**, *30*, 565.
 (20) (a) Brown, G. F.; Stiefel, E. I. *Inorg. Chem.* **1973**, *12*, 2140–2147. (b) Xu, H.-Wu.; Chen, Z.-N.; Wu, J.-G. *Acta Crystallogr., Sect. E* **2002**, *58*, m631. (c) Formitchev, D. V.; Lim, B. S.; Holm, R. H. *Inorg. Chem.* **2001**, *40*, 645–654. (d) Wang, K.; McConnachie, J. M.; Stiefel, E. I. *Inorg. Chem.* **1999**, *38*, 4334–4341. (e) Matsubayashi, G.; Douki, K.; Tamura, H.; Nakano, M.; Mori, W. *Inorg. Chem.* **1993**, *32*, 5990–5996. (f) Draganjac, M.; Coucouvanis, D. *J. Am. Chem. Soc.* **1983**, *105*, 139–140. (g) Smith, A. E.; Schrauzer, G. N.; Mayweg, V. P.; Heinrich, W. *J. Am. Chem. Soc.* **1965**, *87*, 5798. (h) Cowie, M.; Bennett, M. J. *Inorg. Chem.* **1976**, *15*, 1584. (i) Boyde, S.; Garner, C. D.; Enemark, J. H.; Ortega, R. B.; *J. Chem. Soc., Dalton Trans.* **1987**, 2267. (j) Goddard, C. A.; Holm, R. H. *Inorg. Chem.* **1999**, *38*, 5389. (k) Yang, X.; Freeman, G. K. W.; Rauchfuss, T. B.; Wilson, S. R. *Inorg. Chem.* **1991**, *30*, 3034.

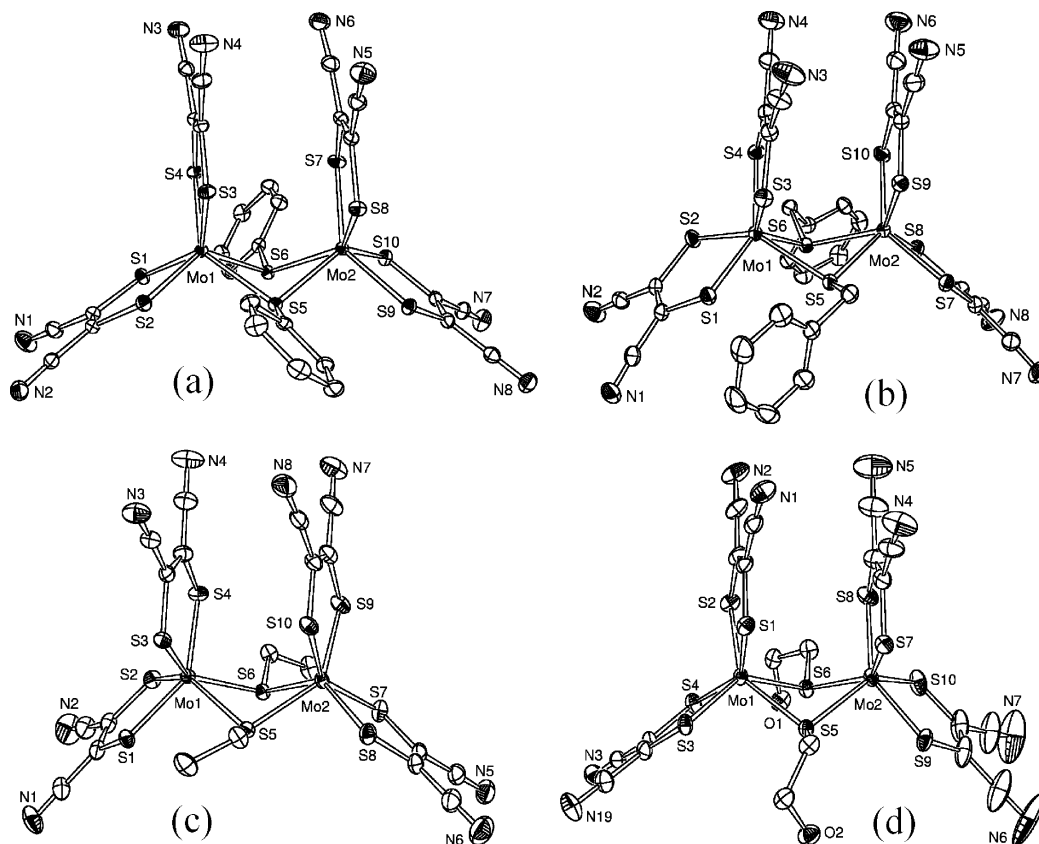


Figure 1. Structure (ORTEP view) of anions of **1** (a), **2** (b), **3** (c), and **4** (d) showing 50% probability thermal ellipsoids. Hydrogen atoms are omitted for clarity.

the reactive $[\text{Et}_4\text{N}]_2\{\text{W}^{\text{IV}}(\text{OH})_2(\text{mnt})_2\}$ species which on responding to dehydration reaction can be reverted back to the starting $\{\text{W}=\text{O}\}$ moiety or may respond to nucleophilic substitution by HSR to change into the desired $\{\text{W}(\text{SR})_2\}$ moiety. Similar chemistry was observed with the molybdenum system. Following this principle, we have thus utilized $[\text{Et}_4\text{N}]_2[\text{Mo}^{\text{IV}}\text{O}(\text{mnt})_2]$ ¹⁴ and $[\text{Et}_4\text{N}]_2[\text{W}^{\text{IV}}\text{O}(\text{mnt})_2]$ ¹⁶ as starting materials to synthesize eight new complexes (Scheme 1). We were interested in exploring a chemistry wherein the formed $[\text{Et}_4\text{N}]_2[\text{M}^{\text{IV}}(\text{SR})_2(\text{mnt})_2]$ ($\text{M} = \text{Mo}/\text{W}$) may have responded to a simple dissociation reaction like $[\text{Et}_4\text{N}]_2[\text{M}^{\text{IV}}(\text{SR})_2(\text{mnt})_2] \rightarrow [\text{Et}_4\text{N}][\text{M}^{\text{IV}}(\text{SR})(\text{mnt})_2] + [\text{Et}_4\text{N}][\text{SR}]$ wherein the all important desoxo pentacoordinated species can be made. However, even in the presence of a lower amount of thiols, the pentacoordinated monomeric species $\{[\text{M}^{\text{IV}}(\text{SR})(\text{mnt})_2]^{-}\}$ dimerized to yield $[\text{Et}_4\text{N}]_2[\text{M}^{\text{IV}}_2(\text{SR})_2(\text{mnt})_4]$ ($\text{M} = \text{Mo}/\text{W}$; $\text{R} = \text{Ph}$ (**1**), CH_2Ph (**2**), CH_2CH_3 (**3**), $\text{CH}_2\text{CH}_2\text{OH}$ (**4**)) (Figures 1 and 2). Such reaction strongly suggests that the pentacoordination did not take place readily, and though it is dimerized, the dimeric forms are devoid of any participation of a M–M

bond, which is so common in pentavalent molybdenum^{12c,21–23}/tungsten^{20j,24} species.

Dimeric Mo(IV) bis(dithiolene) complexes with sulfide, selenide, and phenyl selenide (PhSe^-) as bridging ligand are known,^{12c} but dimeric W(IV) bis(dithiolene) complexes have not been reported yet. In the present approach a new pathway to achieve desoxo Mo(IV)/W(IV) bis(dithiolene) complexes with varying axial ligands has been made. In the complex $[\text{Et}_4\text{N}]_2[\text{M}^{\text{IV}}\text{O}(\text{mnt})_2]$ ($\text{M} = \text{Mo}/\text{W}$), the molybdenyl $\{\text{Mo}^{\text{IV}}=\text{O}\}$ and tungstenyl moieties $\{\text{W}^{\text{IV}}=\text{O}\}$ behaved somewhat like the organic carbonyl group in a sense that the $\text{M}^{\text{IV}}=\text{O}$ ($\text{M} = \text{Mo}/\text{W}$) double bond can be opened up with the addition of acid (HX) to yield $\{\text{M}^{\text{IV}}(\text{OH})(\text{X})\}$ ($\text{M} = \text{Mo}/\text{W}$) and when the counteranion X is mainly a non-coordinating anion like methanesulfonate, the species responded to hydrolysis to yield $\{\text{M}^{\text{IV}}(\text{OH})(\text{OH})\}$ ($\text{M} = \text{Mo}/\text{W}$) moiety.

(21) (a) Shibahara, T.; Iwai, N.; Sasaki, M.; Sakane, G. *Chem. Lett.* **1997**, 445–446. (b) Dilworth, J. R.; Zubietta, J.; Hyde, J. R. *J. Am. Chem. Soc.* **1982**, *104*, 365–367. (c) Mattes, R.; Scholand, H. *Angew. Chem., Int. Ed. Engl.* **1984**, *23*, 382. (d) Mattes, R.; Scholand, H.; Mikloweit, U.; Schrenk, V. *Z. Naturforsch. B: Chem. Sci.* **1987**, *42*, 589–598. (e) Mattes, R.; Scholand, H.; Mikloweit, U.; Schrenk, V. *Z. Naturforsch. B: Chem. Sci.* **1987**, *42*, 599–604. (f) Minelli, M.; Kuhlman, R. L.; Schaffer, S. J.; Chiang, M. Y. *Inorg. Chem.* **1992**, *31*, 3891–3896.

(22) (a) Sung, Kie-Moon.; Holm, R. H. *Inorg. Chem.* **2001**, *40*, 4518, (b) Umakoshi, K.; Nishimoto, E.; Sokolov, M.; Kawano, H.; Sasaki, Y.; Onishi, M. *J. Organomet. Chem.* **2000**, *611*, 370. (c) Young, C. G.; Kocaba, T. O.; Yan, Xue F.; Tiekink, E. R. T.; Wei, L.; Murray, H. H., III; Coyle, C. L.; Stiefel, E. I. *Inorg. Chem.* **1994**, *33*, 6252. (23) (a) Hsieh, T.-C.; Gebreyes, K.; Zubietta, J. *Chem. Commun.* **1984**, 1172–1174. (b) Hsieh, T.-C.; Nicholson, T.; Zubietta, J. *Inorg. Chem.* **1988**, *27*, 241–250. (c) Wall, K. L.; Folting, K.; Huffman, J. C.; Wentworth, R. A. D. *Inorg. Chim. Acta* **1984**, *86*, L25–L27. (d) Bravard, D. C.; Newton, W. E.; Huneke, J. T.; Yamanouchi, K.; Enemark, J. H. *Inorg. Chem.* **1982**, *21*, 3795–3798. (24) (a) Yifan, Zheng; Nianyong, Zhu; Huqiang, Zhan; Xintao, Wu. *Acta Crystallogr., Sect. C* **1989**, *45*, 1632–1633. (b) Sellmann, D.; Weiss, R.; Knoch, F. *Inorg. Chim. Acta* **1990**, *175*, 65–75. (c) Sellmann, D.; Kern, W.; Pohlmann, G.; Knoch, F.; Moll, M. *Inorg. Chim. Acta* **1991**, *185*, 155–162.

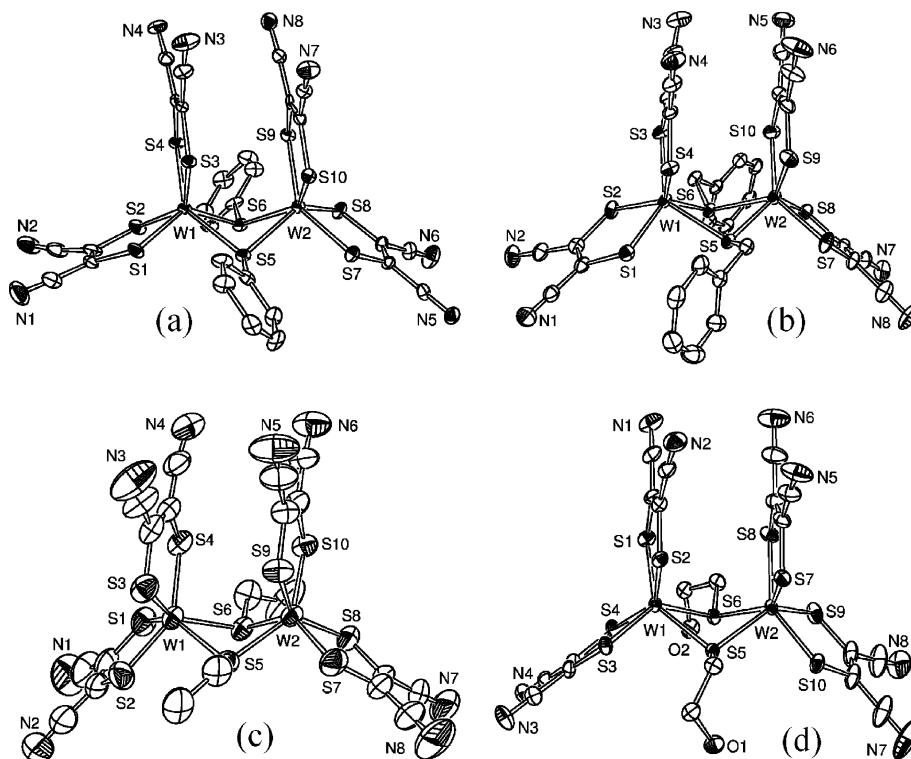
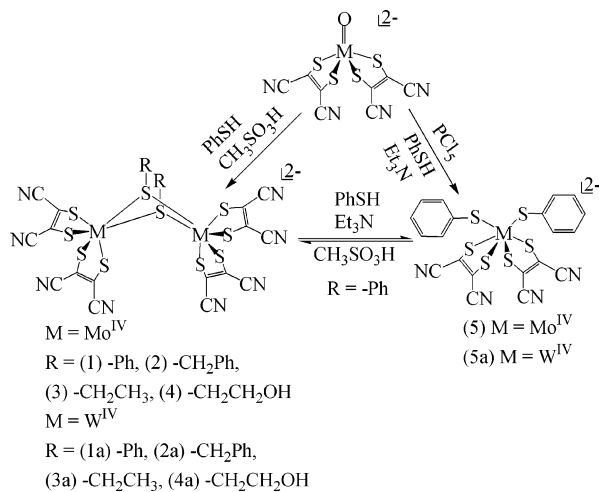


Figure 2. Structure (ORTEP view) of anions of **1a** (a), **2a** (b), **3a** (c), and **4a** (d) showing 50% probability thermal ellipsoids. Hydrogen atoms are omitted for clarity.

Scheme 1. Synthesis of Desoxo Molybdenum and Tungsten Complexes and Interconversion between the Dimeric and Monomeric Form (when R = -Ph)



Such species are very reactive intermediates to respond to nucleophilic reactions with thiols. On the basis of this chemistry, the treatment of [Et₄N]₂[M^{IV}O(mnt)₂] (M = Mo/W) with 4 equiv of different thiols in the presence of methanesulfonic acid resulted in the formation of respective dimeric complexes in 85% yield, where both the metal atoms retained the oxidation state of IV. Due to the acidic pH, the deprotonation of thiol is largely suppressed, resulting in a lower number of thiols accessible by metal centers thus facilitating the dimerization of the pentacoordinated complexes. The monomeric tungsten complex (**5a**) has been synthesized (Scheme 1) following the reported method for the synthesis of **5**,¹⁵ where PCl₅ was used to open up the

{Mo=O} bond to yield an unstable intermediate {Mo(Cl)₂}, and upon addition of Et₃N, the thiols got ligated with the release of [Et₃NH][Cl] leading to the formation of **5**. The bridging thiolate groups in all the dimeric complexes can be opened up easily with the formation of a reactive intermediate in dichloromethane medium. Traces of water present in the solvent is capable of hydrolyzing the complex back to the starting material at room temperature. Interestingly, in polar solvents like acetonitrile, DMSO, or DMF, these dimers are converted into the well-known [Et₄N]₂[M^{IV}(mnt)₃]^{20,12c} (M = Mo/W). Such behavior of these complexes in nonpolar and polar solvents demonstrated not only the tendency of the bridging thiols to dissociate but also the increased lability of the coordinated dithiolene moiety in polar solvents. Such dissociation of dithiolene (mnt) in forming the tris complex directly indicates the inherent chemistry associated with the long known reconstitution assay of a specific molybdenum cofactor with the nit-1 mutant of *Neurospora crassa* to create active nitrate reductase. The dissociation of thiolate ligands has also been reported in the case of bis-molybdopterin enzymes of the DMSOR family, which has been shown not to be a part of the catalytic cycle.²³ The native dissimilatory nitrate reductase (*Desulfovibrio desulfuricans*)¹¹ uses its lone Cys140 (from domain III) to coordinate molybdenum cofactor to acquire pentacoordination, a requirement of the active site. Our sincere attempts to synthesize monothiolate ligation of the {M^{IV}(mnt)₂} (M = Mo/W) moiety was thwarted by the drive of the active pentacoordinated species to dimerize instantaneously attaining a stable hexacoordination. A similar dimerization process was encountered in the reaction between

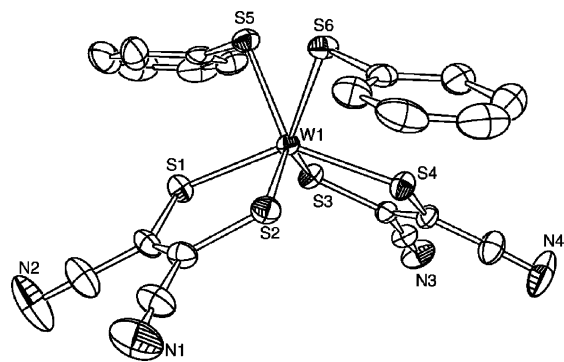


Figure 3. Structure (ORTEP view) of the anion of **5a** showing 50% probability thermal ellipsoids. Hydrogen atoms are omitted for clarity.

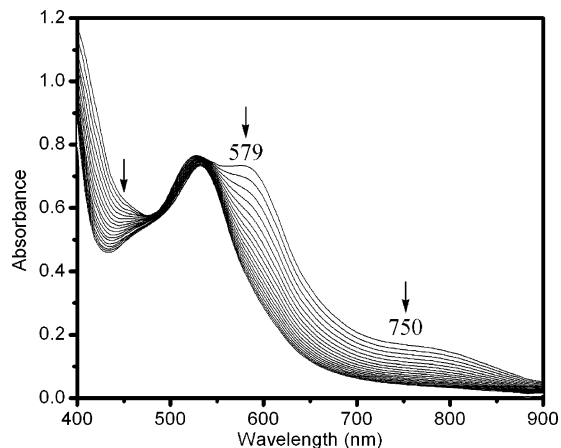


Figure 4. Conversion of $[\text{Et}_4\text{N}]_2[\text{Mo}^{\text{IV}}_2(\text{SPh})_2(\text{mnt})_4]$ to $[\text{Et}_4\text{N}]_2[\text{Mo}^{\text{IV}}(\text{SPh})_2(\text{mnt})_2]$ in dichloromethane. Concentration of $[\text{Et}_4\text{N}]_2[\text{Mo}^{\text{IV}}_2(\text{SPh})_2(\text{mnt})_4] = 1 \times 10^{-4}$ M; concentration of $\text{Et}_3\text{N} = 1$ M. Total time = 85 min. Scan rate = 5 min/scan.

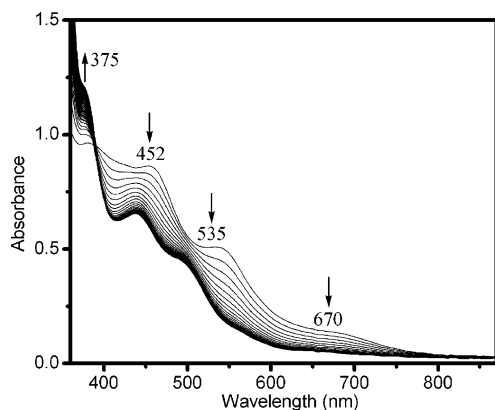


Figure 5. Conversion of $[\text{Et}_4\text{N}]_2[\text{W}^{\text{IV}}_2(\text{SPh})_2(\text{mnt})_4]$ to $[\text{Et}_4\text{N}]_2[\text{W}^{\text{IV}}(\text{SPh})_2(\text{mnt})_2]$ in dichloromethane. Concentration of $[\text{Et}_4\text{N}]_2[\text{W}^{\text{IV}}_2(\text{SPh})_2(\text{mnt})_4] = 1 \times 10^{-4}$ M; concentration of $\text{Et}_3\text{N} = 1$ M. Total time = 96 min. Scan rate = 2 min/scan.

$[\text{Mo}^{\text{IV}}(\text{CO})_2(\text{S}_2\text{C}_2\text{Ph}_2)_2]$ and Et_4NSePh , which was finally achieved by the use of a sterically bulky selenolate ligand.^{12c} The apoprotein functions as a lone thiol (Cys140) donor and sterically protects the monomeric molybdenum center to prevent dimerization. However, in CO dehydrogenase, its apoprotein accommodates a hetero-bimetallic molybdenum–copper cofactor in its active site.²⁶

(25) Bray, R. C.; Adams, B.; Smith, A. T.; Bennet, B.; Bailey, S. *Biochemistry* **2000**, *39*, 11258–11269.

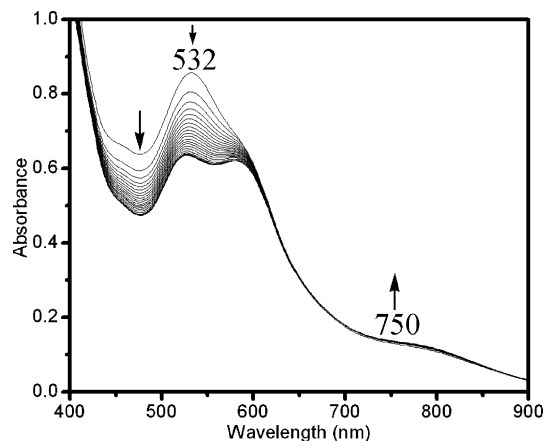


Figure 6. Conversion of $[\text{PPh}_4]_2[\text{Mo}^{\text{IV}}(\text{SPh})_2(\text{mnt})_2]$ to $[\text{PPh}_4]_2[\text{Mo}^{\text{IV}}_2(\text{SPh})_2(\text{mnt})_4]$ in dichloromethane. Concentration of $[\text{PPh}_4][\text{Mo}^{\text{IV}}(\text{SPh})_2(\text{mnt})_2] = 2 \times 10^{-4}$ M; concentration of $\text{CH}_3\text{SO}_3\text{H} = 2 \times 10^{-4}$ M. Total time = 220 min. Scan rate = 10 min/scan.

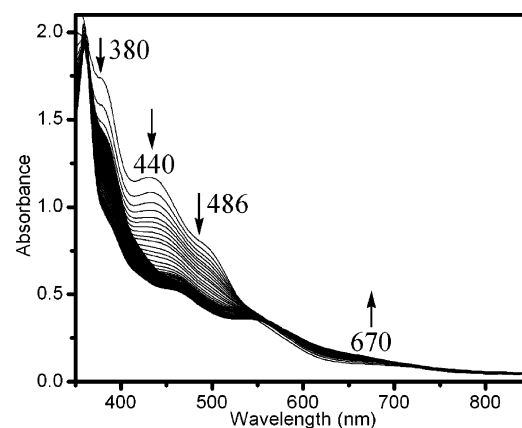
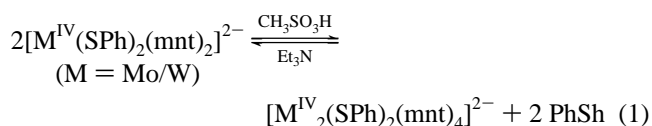


Figure 7. Conversion of $[\text{PPh}_4]_2[\text{W}^{\text{IV}}(\text{SPh})_2(\text{mnt})_2]$ to $[\text{PPh}_4]_2[\text{W}^{\text{IV}}_2(\text{SPh})_2(\text{mnt})_4]$ in dichloromethane. Concentration of $[\text{PPh}_4][\text{W}^{\text{IV}}(\text{SPh})_2(\text{mnt})_2] = 2 \times 10^{-4}$ M; concentration of $\text{CH}_3\text{SO}_3\text{H} = 3 \times 10^{-4}$ M. Total time = 60 min. Scan rate = 30 s/scan.

pH-Dependent Interconversion between the Dimeric and Monomeric Species. Dimeric complex of molybdenum or tungsten may be converted into the corresponding monomeric bis(dithiolene) M(IV) dithiol complex ($\text{M} = \text{Mo}/\text{W}$) upon addition of the base like Et_3N in the presence of a minimum of 2 equiv of thiols. Curiously, the monomeric bis(dithiolene) M(IV) dithiol complex ($\text{M} = \text{Mo}/\text{W}$) is reverted back to the corresponding dimeric complex upon addition of $\text{CH}_3\text{SO}_3\text{H}$, as shown in the representative reaction (eq 1):



The dimeric complex can be converted back into its corresponding monomeric complex, even in the absence of thiols, but only under basic condition (eq 2). This clearly indicates that the opening of the thiol bridge is facilitated in

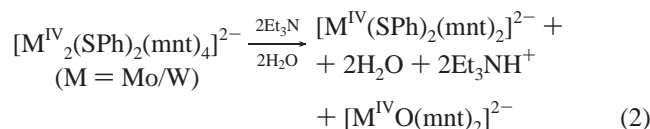
(26) (a) Gnida, M.; Ferner, R.; Gerner, L.; Meyer, O.; Meyer-Klaucke, W. *Biochemistry* **2003**, *42*, 222–230. (b) Dobbek, H.; Gremer, L.; Kiefersauer, R.; Huber, R.; Meyer, O. *Proc. Natl. Acad. Sci.* **2002**, *99*, 15971–15976.

Table 1. Crystallographic Data^a for Complexes 1–4

complexes	1	2	3	4
formula	Mo ₂ S ₁₀ C ₄₄ N ₁₀ H ₅₀	Mo ₆ S ₃₀ C ₁₄₂ N ₃₂ H ₁₄₂	Mo ₂ S ₁₀ C ₃₆ N ₁₀ H ₅₀	Mo ₂ S ₁₀ C ₃₆ N ₁₀ H ₅₀ O ₂
fw	1231.42	3834.62	1135.44	1167.44
cryst syst	triclinic	monoclinic	monoclinic	monoclinic
space group	<i>P</i> 1	<i>P</i> 2 ₁ / <i>c</i>	<i>P</i> 2 ₁ / <i>c</i>	<i>P</i> 2 ₁ / <i>c</i>
<i>T</i> , K	100	100	100	100
<i>Z</i>	2	4	4	4
<i>a</i> , Å	11.824 (5)	20.596 (5)	19.419 (5)	19.542 (5)
<i>b</i> , Å	14.496 (5)	18.049 (5)	14.377 (5)	14.284 (5)
<i>c</i> , Å	16.500 (5)	46.838 (5)	19.308 (5)	19.587 (5)
α, deg	98.803 (5)	90.000 (5)	90.000 (5)	90.000 (5)
β, deg	109.364 (5)	94.498 (5)	114.375 (5)	113.128 (5)
γ, deg	92.968 (5)	90.000 (5)	90.000 (5)	90.000 (5)
<i>V</i> , Å ³	2620.7 (16)	17358 (7)	4910 (2)	5028 (3)
<i>d</i> _{calcd} , g/cm ³	1.561	1.477	1.536	1.542
μ, mm ⁻¹	0.920	0.837	0.974	0.957
Θ range, deg	2.12–28.27	2.04–28.34	2.12–28.33	2.27–28.37
GOF (<i>F</i> ²)	1.031	1.045	1.030	1.078
R1 ^b (wR2 ^c)	0.0340 (0.0824)	0.0558 (0.1218)	0.0414 (0.0920)	0.0678 (0.1344)

^a Mo Kα radiation. ^b R1 = Σ||*F*₀ − |*F*_c||/Σ|*F*₀|. ^c wR2 = {Σ[*w*(*F*₀² − *F*_c²)]/Σ[*w*(*F*₀²)]}^{1/2}.

basic pH, which leads to monomeric bis(dithiolene) M(IV) dithiol (M = Mo/W) complex and the naked {M(IV)bis(dithiolene)}(M = Mo/W) moiety, which being an avid oxophile, abstracts oxygen from the traces of moisture present in the reaction medium to yield [M^{IV}O(mnt)₂]^{2−} (M = Mo/W) (eq 2) :



It is interesting to note that pH-dependent monomer-to-dimer conversion is apparently faster in the case of tungsten complexes, as seen in the conversion of **5a** to **1a** (Figure 7) than that in molybdenum complexes as seen for the corresponding conversion of **5** to **1** (Figure 6). The *K*_{eq} (Mo) for the conversion of **5** to **1** (monomer to dimer) as in eq 1 has been found to be (3.6 ± 1) × 10³ M⁻¹, and for the conversion of **5a** to **1a** in tungsten systems, the corresponding *K*_{eq}(W) value is (7.4 ± 1) × 10³ M⁻¹. Reactions 1 and 2 may be used to draw an analogy to the close relationship between the oxo and desoxo types of Mo cofactors present in the same family of molybdoenzymes.

Dimer–monomer interconversion in Mo(IV)/W(IV) bis(dithiolene) complexes demonstrates the utility of dithiolene moiety in stabilizing the Mo(IV) complexes as in the active sites of native enzymes. This interconversion also establishes the fact that even if the pentacoordinated Mo(IV) and W(IV) bis(dithiolene) moieties are forced to dimerize, they can be reverted back easily to the corresponding monomeric entity. Attempts to synthesize monomeric complexes corresponding to **2**, **3**, **4**, and their tungsten analogues have not been successful due to their high susceptibility toward hydrolysis. However, the conversion of dimers to monomers can be utilized to prepare hitherto unknown monomeric bis(dithiolene) M(IV) mixed dithiol complexes (M = Mo/W).

X-ray Structure Description. All nine complexes are characterized by X-ray structure determination. Structures are shown in Figure 1–3, and the leading structural

parameters are collected in Tables 1 and 2. The selected bond distances and angles are presented in Tables 3–6. For the most part, these parameters are in good agreement with the other related molybdenum bis(dithiolene) complexes.^{14,15} Mo(IV)^{12c,27} and W(IV)^{20j,24} dimeric complexes have been reported earlier. All eight complexes (**1–4** and **1a–4a**) reported in this paper exhibit two six-coordinate trigonal prismatic units bridged by two common thiolate sulfur atom with no metal–metal bond leading to a nonplanar rhomboidal bridge. Each trigonal prismatic unit is comprised of two bidentate malenonitriledithiolate and two thiolate molecules. The ranges of mean C–C and S–C bond distances are 1.33–1.34 and 1.73–1.79 Å, respectively, which are sufficiently close to the typical bond lengths (sp²)C=C(sp²) = 1.331(9) Å and S–C(sp²) = 1.75(2) Å to establish the ligand mnt²⁸ as a classical ene-1,2-dithiolate, as observed in other reported bis(dithiolene) molybdenum complexes. There are considerable variations in the Mo–S (thiolate) bond distances and Mo–S–Mo angles within the series (**1–4**). The large Mo–S (thiolate) bond distances ranging from 2.428(1) to 2.484(1) Å are not unprecedented,²² but much larger than Mo–S (thiolate) bond distances in synthetic complexes reported earlier.^{12c,21b} The average Mo–S (thiolate) bond distances are 2.473 (**1**), 2.457 (**2**), 2.458 (**3**), and 2.449 Å (**4**). The longest bond distance occurs in the case of **1**, explaining the fact that complex **1** is the most unstable one toward thiol dissociation. The shortest Mo–S–Mo angle in the series ranging from 92.84(2)° to 93.01(3)°, arises in complex **1**, whereas in the other three complexes (**2**, **3**, **4**), the same angle ranges from 94.30(5)° to 95.71(4)°. These angles are much greater than that reported (ranging from 70–80°) in the case of the complexes containing a Mo–Mo single bond.^{12c,22a,b,23} This is also consistent with the distance between two molybdenum centers which is lowest (3.586 Å) in the case

(27) Hsu, H.-F.; Peng, W.-Y.; Li, Z.-Y.; Wu, R.-R.; Liao, J.-H.; Wang, Y.; Liu, Y.-H.; Shieh, M.; Kuo, T.-S. *Inorg. Chim. Acta* **2005**, *358*, 2149–2154.

(28) Bahr, G.; Schlettzer, B. *Ber.* **1955**, *88*, 1771. (b) Bahr, G. *Angew. Chem.* **1956**, *68*, 525. (c) Stiefel, E. I.; Bennet, L. E.; Dori, Z.; Crawford, T. H.; Simo, C.; Gray, H. B. *Inorg. Chem.* **1970**, *9*, 281–286. (d) Davidson, A.; Holm, R. H. *Inorg. Synth.* **1967**, *10*, 8.

Table 2. Crystallographic Data^a for Complexes **1a–4a**

complexes	1a	2a	3a	4a
formula	W ₂ S ₁₀ C ₄₄ N ₁₀ H ₅₀	W ₂ S ₁₀ C ₄₆ N ₁₀ H ₅₄	W ₂ S ₁₀ C ₃₆ N ₁₀ H ₅₀	W ₂ S ₁₀ C ₃₆ N ₁₀ H ₅₀ O ₂
fw	1407.32	1435.37	1311.24	1343.24
cryst syst	monoclinic	triclinic	monoclinic	monoclinic
space group	<i>C2/c</i>	<i>P1</i>	<i>P2₁/c</i>	<i>P2₁/c</i>
<i>T</i> , K	100	100	100	100
<i>Z</i>	8	2	4	4
<i>a</i> , Å	28.897 (5)	11.332 (5)	19.570 (5)	19.545 (5)
<i>b</i> , Å	11.481 (5)	15.089 (5)	14.516 (5)	14.274 (5)
<i>c</i> , Å	33.556 (5)	18.625 (5)	19.563 (5)	19.548 (5)
α , deg	90.000 (5)	101.109 (5)	90.000	90.000 (5)
β , deg	94.246 (5)	98.540 (5)	113.94 (5)	113.289 (5)
γ , deg	90.000 (5)	97.958 (5)	90.000	90.000 (5)
<i>V</i> , Å ³	11102 (5)	3044.2 (9)	5079 (3)	5009 (3)
<i>d</i> _{calcd.} , g/cm ³	1.684	1.566	1.715	1.781
μ , mm ⁻¹	4.558	4.157	4.974	5.049
Θ range, deg	1.99–28.30	2.27–28.31	2.09–28.40	2.10–28.33
GOF (<i>F</i> ²)	1.039	1.036	1.047	1.013
R1 ^b (wR2 ^c)	0.0516 (0.1074)	0.0362 (0.0885)	0.0632 (0.1361)	0.0357 (0.0827)

^a Mo K α radiation. ^b R1 = $\sum||F_o| - |F_c||/\sum|F_o|$. ^c wR2 = $\{\sum[w(F_o^2 - F_c^2)^2]/\sum[w(F_o^2)^2]\}^{1/2}$.

Table 3. Selected Bond Distances (Å) for Complexes **1–4**

distances	1	2	3	4
Mo(1)–Mo(2)	3.586	3.641	3.635	3.610
Mo(1)–S(5)	2.463 (9)	2.449 (1)	2.453 (8)	2.445 (1)
Mo(1)–S(6)	2.480 (9)	2.460 (1)	2.459 (9)	2.428 (1)
Mo(1)–S(6)	2.466 (9)	2.461 (1)	2.444 (9)	2.478 (1)
Mo(2)–S(6)	2.484 (1)	2.455 (1)	2.476 (8)	2.445 (1)

Table 4. Selected Angles (deg) for Complexes **1–4**

angles	1	2	3	4
Mo(1)–S(5)–Mo(2)	93.01 (3)	95.71 (4)	95.46 (3)	95.59 (5)
Mo(1)–S(6)–Mo(2)	92.84 (2)	95.52 (4)	95.24 (3)	94.30 (5)
dihedral angle ^a	73.72	69.22	67.29	69.62

^a Angle between two planes containing Mo(1), S(5), Mo(2) and Mo(1), S(6), Mo(2), respectively.

Table 5. Selected Bond Distances (Å) for Complexes **1a–4a**

distances	1a	2a	3a	4a
W(1)–W(2)	3.520	3.644	3.641	3.605
W(1)–S(5)	2.458 (1)	2.451 (1)	2.469 (2)	2.434 (1)
W(2)–S(5)	2.468 (1)	2.462 (1)	2.441 (3)	2.418 (1)
W(1)–S(6)	2.446 (1)	2.460 (1)	2.449 (2)	2.467 (1)
W(2)–S(6)	2.456 (1)	2.455 (1)	2.442 (2)	2.444 (1)

Table 6. Selected Angles (deg) for Complexes **1a–4a**

angles	1a	2a	3a	4a
W(1)–S(5)–W(2)	91.20 (5)	95.72 (4)	95.72 (8)	95.95 (4)
W(1)–S(6)–W(2)	91.76 (6)	95.67 (4)	96.25 (8)	94.44 (4)
dihedral angle ^a	77.23	67.32	67.27	69.01

^a Angle between two planes containing W(1), S(5), W(2) and W(1), S(6), W(2), respectively.

of complex **1** but ranges from 3.610–3.641 Å in complexes **2–4**. A Mo–Mo bond is nonexistent in these complexes reported here as revealed in the large distance maintained between two molybdenum centers compared to those with Mo–Mo single bond (ranging from 2.660 to 3.023 Å) reported earlier^{12c,21–23} and also from the fact that the complexes are EPR inactive as expected for Mo(IV) bis-(dithiolene) complexes^{14,15,29,8a,b} reported earlier. However, these distances are somewhat shorter than the Mo–Mo distance of 3.858 Å reported earlier^{12c} in the case of binuclear Mo(IV) complexes with bridging phenylselenides containing

Table 7. Redox Potentials for Complexes **1–4** (CV and DPP)

complexes	<i>E</i> _{pc} (V)	ΔE _{pp} (mV)	<i>E</i> _{1/2} (V)	<i>E</i> _{1/2} (V) from DP	<i>I</i> _{pa} / <i>I</i> _{pc}
1	0.774 ^a 1.130 ^{i,a}	78 –	0.813 –	0.787 1.039	0.72 –
2	0.743 ^a 0.969 ^{i,a}	73 –	0.779 –	0.813 1.041	1.24 –
3	0.750 ^a 1.108 ^{i,a}	74 –	0.787 –	0.810 1.088	1.09 –
4	0.897 ^{i,b}	–	–	0.898	–

^a Measured in dichloromethane at 100 mV/s. ^b Measured in acetonitrile at 100 mV/s. i = irreversible

Table 8. Redox Potentials for Complexes **1a–5a** (CV and DPP)

complexes	<i>E</i> _{pc} (V)	ΔE _{pp} (mV)	<i>E</i> _{1/2} (V)	<i>E</i> _{1/2} (V) from DP	<i>I</i> _{pa} / <i>I</i> _{pc}
1a	0.616 ^a 0.941 ^{i,a}	84 –	0.658 –	0.713 0.944	1.26 –
2a	0.595 ^a 0.929 ^{i,a}	91 –	0.640 –	0.686 0.932	1.24 –
3a	0.601 ^a 0.995 ^{i,a}	86 –	0.644 –	0.670 0.959	1.48 –
4a	0.742 ^{i,b}	–	–	0.746	–
5a	0.011 ^a 0.682 ^{i,a}	69 –	0.045 –	0.063 0.660	1.03 –

^a Measured in dichloromethane at 100 mV/s. ^b Measured in acetonitrile at 100 mV/s. i = irreversible

no metal–metal bond. The dihedral angle between the planes containing Mo(1), S(5), Mo(2) and Mo(1), S(6), Mo(2) is lowest (67.28°) in the case of **3** and highest (73.71°) in the case of **1**.

There are considerable variations in the W–S (thiolate) bond distances and W–S–W angles within the series (**1a–4a**). W–S (thiolate) bond distances ranging from 2.418(1)

- (29) (a) Boyde, S.; Ellis, S. R.; Garner, C. D.; Clegg, W. *J. Chem. Soc., Chem. Commun.* **1986**, 1483–1485. (b) Davies, E. S.; Beddoes, R. L.; Collison, D.; Dinsmore, A.; Docrat, A.; Joule, J. A.; Wilson, C. R.; Garner, C. D. *J. Chem. Soc. Dalton Trans.* **1997**, 21, 3985. (c) Oku, H.; Ueyama, N.; Kondo, M.; Nakamura, A. *Inorg. Chem.* **1994**, 33, 209–216. (d) Ansari, M. A.; Chandrasekaran, J.; Sarkar, S. *Inorg. Chim. Acta* **1987**, 133, 133–136. (e) Matsubayashi G.; Nojo, T.; Tanaka, T. *Inorg. Chim. Acta* **1988**, 154, 133–135. (f) Götze, B.; Knoch, F.; Kisch, H. *Chem. Ber.* **1996**, 129, 33–37. (g) McCleverty, J. A.; Locke, J.; Ratcliff, B.; Wharton, E. *J. Inorg. Chim. Acta* **1969**, 3, 283–286.523.

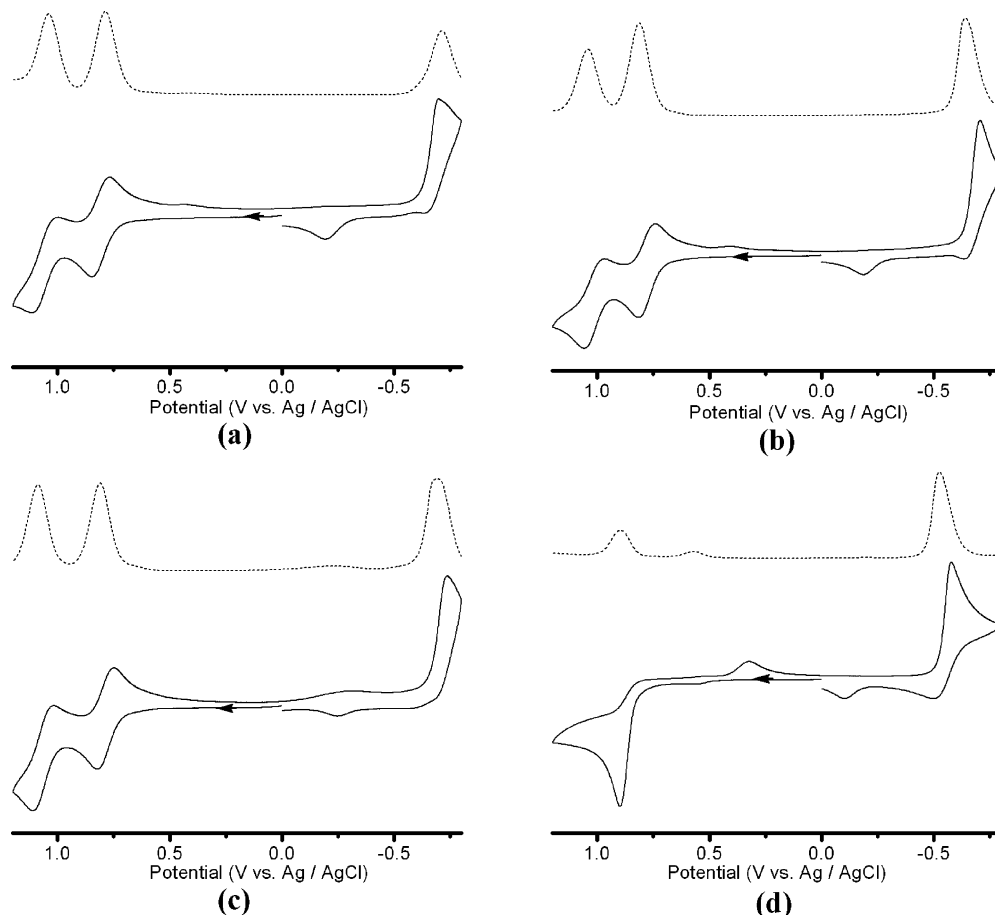


Figure 8. Cyclic voltametric traces (scan rate = 100 mV/s) and differential pulse polarographs (scan rate = 20 mV/s, pulse width = 50 ms, pulse period = 200 ms, pulse amplitude = 50 mV) of the synthesized complexes. (a) $[\text{Et}_4\text{N}]_2[\text{Mo}^{\text{IV}}_2(\text{SPh})_2(\text{mnt})_4]$, (b) $[\text{Et}_4\text{N}]_2[\text{Mo}^{\text{IV}}_2(\text{SCH}_2\text{Ph})_2(\text{mnt})_4]$, (c) $[\text{Et}_4\text{N}]_2[\text{Mo}^{\text{IV}}_2(\text{SCH}_2\text{CH}_3)_2(\text{mnt})_4]$ in dichloromethane, and (d) $[\text{Et}_4\text{N}]_2[\text{Mo}^{\text{IV}}_2(\text{SCH}_2\text{CH}_2\text{OH})_2(\text{mnt})_4]$ in acetonitrile.

to 2.469(2) Å are much larger than W–S (thiolate) bond distances ranging from 2.321 to 2.346 Å in some of the dimeric tungsten(V) complexes reported earlier.^{20j,24} The average W–S (thiolate) bond distances are 2.457 (1a), 2.457 (2a), 2.450 (3a), and 2.441 Å (4a). W–S–W angles are much larger in complexes 1a–4a than in complexes (78.50–79.84°) reported earlier.^{20j,24} The shortest W–S–W angle in the series, ranging from 91.20(5)° to 91.76(6)°, arises in complex 1a whereas in the other three complexes (2a, 3a, 4a), the same angle ranges from 94.44(4)° to 96.25–(8)°. This is consistent with the distance between two tungsten centers, which is lowest (3.520 Å) in the case of complex 1a, but ranges from 3.605 to 3.644 Å in complexes 2a–4a. A W–W bond is nonexistent in these complexes reported here as revealed in the large distance maintained between two tungsten centers compared to those with a W–W single bond (ranging from 2.791 to 3.013 Å) reported earlier.^{20j,24} The dihedral angle between the planes containing W(1), S(5), W(2) and W(1), S(6), W(2) is lowest (67.27°) in the case of 3a and highest (77.23°) in the case of 1a.

The phenyl rings of thiophenols in 1 and 1a are directed in opposite directions and are almost perpendicular to each other to get relief of steric congestion. This situation does not arise in the other six complexes where there is(are) spacer methylene group(s). As a result of that, two phenyl rings of

benzylthiol (in the case of 2 and 2a), $-\text{CH}_2\text{CH}_3$ (in the case of 3 and 3a), and the $-\text{CH}_2\text{OH}$ moiety (in the case of 4 and 4a) are directed in the same face but toward opposite directions and are only slightly deviated from parallel disposition.

Unlike the equal distance of 2.429 Å for both the W–S(thiophenolate) bond in a reported complex,^{24a} tetraethylammonium bis(but-2-ene-2,3-dithiolato-*S,S'*)-bis(phenylthiolato)-tungsten(V), complex 5a (Figure 3) exhibits a W–S(thiophenolate) distance of 2.426 Å in the case of W–S(5) and 2.441 Å in the case of W–S(6) (see Supporting Information for structural parameters). Two phenyl rings are directed in opposite directions with a S(5)–W(1)–S(6) angle of 72.14° which is much less than that (86°) reported earlier.^{24a} The distance (2.865 Å) between S(5) and S(6) in 5a is much less than that reported earlier (3.313 Å) in a W(V) complex.^{24a} This small distance suggests a weak interaction between the two thiophenolate sulfur atoms which might be the cause for the lability of W–SPh bond, which facilitates conversion of 5a to the dimeric form (1a).

UV–Vis Spectroscopic Measurements. Electronic spectral measurement of the complexes (1, 2, 3, 1a, 2a, 3a) were recorded in dichloromethane (see Supporting Information). Due to less solubility in dichloromethane, electronic spectral measurement of the complexes 4 and 4a were recorded in acetonitrile (see Supporting Information). The absorption

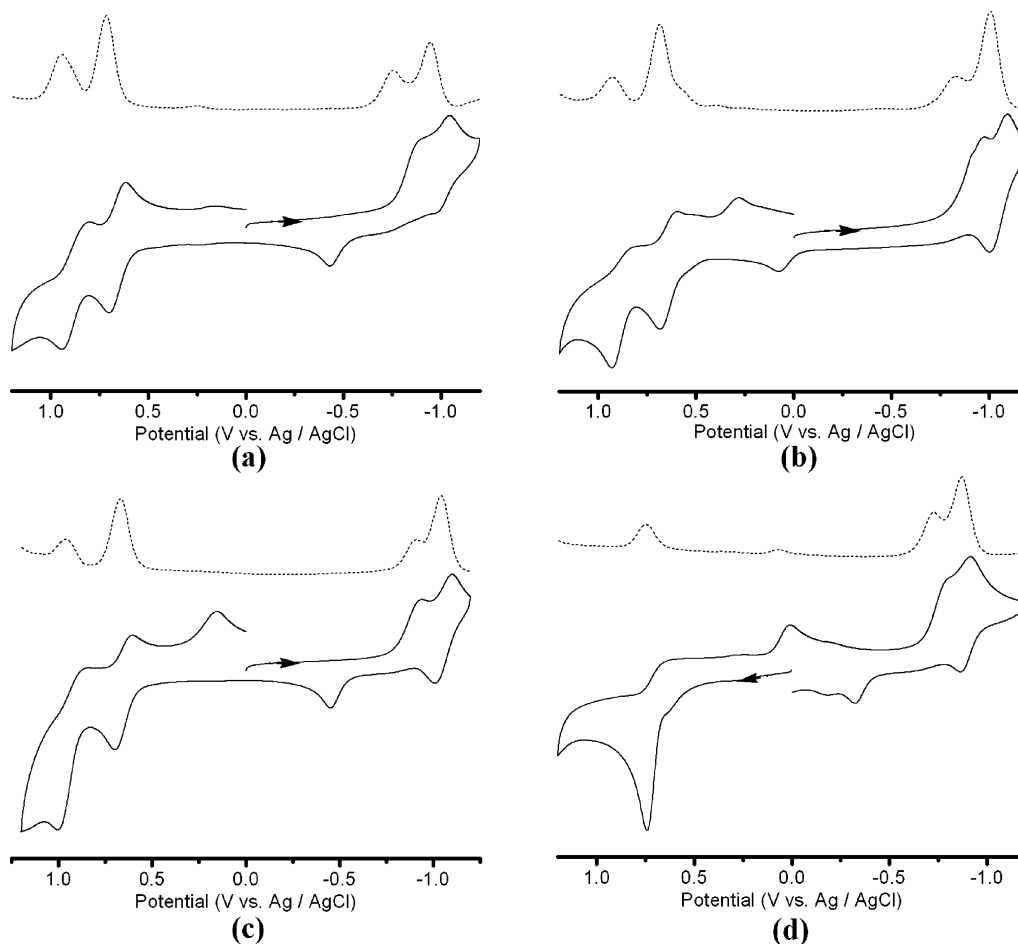


Figure 9. Cyclic voltametric traces (scan rate = 100 mV/s) and differential pulse polarographs (scan rate = 20 mV/s, pulse width = 50 ms, pulse period = 200 ms, pulse amplitude = 50 mV) of the synthesized complexes. (a) $[\text{Et}_4\text{N}]_2[\text{W}^{\text{IV}}_2(\text{SPh})_2(\text{mnt})_4]$, (b) $[\text{Et}_4\text{N}]_2[\text{W}^{\text{IV}}_2(\text{SCH}_2\text{Ph})_2(\text{mnt})_4]$, (c) $[\text{Et}_4\text{N}]_2[\text{W}^{\text{IV}}_2(\text{SCH}_2\text{CH}_3)_2(\text{mnt})_4]$ in dichloromethane, and (d) $[\text{Et}_4\text{N}]_2[\text{W}^{\text{IV}}_2(\text{SCH}_2\text{CH}_2\text{OH})_2(\text{mnt})_4]$ in acetonitrile.

spectral feature is the same for complexes **2**, **3**, and **4**, which showed one distinct peak around ~ 516 nm along with a shoulder around ~ 565 nm. In **1** two distinctive absorption bands of nearly the same intensity at 522 and 579 nm were observed. Molybdenum dimeric complexes show a broad band around ~ 750 nm which can be treated as a common characteristic for this type of thiol-bridged Mo(IV) dimers. Absorption spectral features are the same (see Supporting Information) for complexes **2a**, **3a**, and **4a**, which showed two absorption bands around ~ 416 and ~ 525 nm. In **1a** two distinctive absorption bands at 452 and 535 nm were observed. Tungsten dimeric complexes show a broad band around ~ 670 nm which can be treated as a common characteristic for this type of thiol-bridged W(IV) dimers. Complex **5a** showed two absorption bands at 380 and 440 nm along with two shoulders at 486 and 555 nm and a broad band near 704 nm (see Supporting Information). The conversion of molybdenum and tungsten dimeric complexes to the tris complex, $[\text{Et}_4\text{N}]_2[\text{M}^{\text{IV}}(\text{mnt})_3]$ ($\text{M} = \text{Mo}/\text{W}$) has been studied by UV-vis spectroscopy (see Supporting Information), which shows that the tungsten dimers are relatively more stable toward ligand dissociation in polar solvents like acetonitrile. The pH-dependent conversions of dimers to monomers have been monitored by UV-vis spectroscopy, which with the representative complexes **1** and

1a are shown in Figures 4 and 5, respectively. The pH-dependent conversions of monomers to dimers have also been monitored by UV-vis spectroscopy, which with the representative complexes **1** and **1a** are shown in Figures 6 and 7, respectively.

Electrochemistry. The electrochemical properties of these dimeric complexes were investigated by cyclic voltammetry and by differential pulse polarography (Figures 8 and 9), and the results are summarized in Tables 7 and 8. Due to poor solubility in dichloromethane, cyclic voltammetry and differential pulse polarography of complex **4** and **4a** were performed in acetonitrile. Complexes **1**, **2**, and **3** exhibited one quasi-reversible oxidation at $E_{1/2} = 0.813$, 0.779, and 0.787 V, respectively. All of these exhibited one additional oxidation at 1.039, 1.041, and 1.088 V, respectively. Complexes **1a**, **2a**, and **3a** exhibited one quasi-reversible oxidation at $E_{1/2} = 0.658$, 0.640, and 0.644 V, respectively. One additional oxidation was observed at 0.941, 0.929 and 0.995 V respectively. We could not perform coulometric analysis of these complexes due to a pre-adsorption process on the platinum electrode with time, nevertheless, ΔE_{pp} values (Table 2) and the similar current response using ferrocene (Fc) as internal standard at the same concentration suggest that these quasi-reversible processes are one-electron oxidation processes. The two sequential one-electron oxida-

tion steps could be associated with the oxidation of the molybdenum/tungsten centers from Mo(IV)/W(IV) to Mo(V)/W(IV), and in that case the participation of the odd electron available in each Mo(V)/W(V) to create a Mo(V)–Mo(V)/W(V)–W(V) metal–metal bond would have been a possibility. In such a case the second oxidation step near 1.00 V should be completely irreversible. The quasi-reversible nature of the second step in oxidation clearly showed a different electronic population where the metal orbitals no longer remain discrete. Complexes **4** and **4a** behaved differently in this respect, which showed only one irreversible oxidation at 0.897 and 0.742 V, respectively. This could be due to their instability in a polar solvent like acetonitrile. Complex **5a** exhibits one reversible oxidation at $E_{1/2} = 0.045$ V and one irreversible oxidation at 0.682 V (see Supporting Information).

Conclusion

This paper describes the synthesis, characterization, and comparative chemical, as well as structural, analysis of a new series of dimeric bis(dithiolene) Mo(IV) and W(IV) complexes and one monomeric bis(dithiolene) tungsten bis-(thiophenolate) complex. The dimeric complexes exhibit no metal–metal bond, although two bis(dithiolene) M(IV) (M = Mo/W) moieties are attached together by two thiolate bridges. This bridge formation has been shown to be reversible by the fact that molybdenum and tungsten dimeric complexes can be converted to their corresponding mono-

meric complexes and vice versa upon change in pH. Dimer–monomer interconversion in Mo(IV)/W(IV) bis(dithiolene) complexes establishes the fact that even if the pentacoordinated Mo(IV) and W(IV) bis(dithiolene) moieties, under depleted thiol, are forced to dimerize, they can easily be reverted back to the monomeric unit. Formation of these dimeric complexes and the pH-dependent interconversion between dimeric and monomeric species described herein conveyed the message that the sixth coordination site requires a ligand as a blocker which on demand can make room for other suitable substrates to coordinate leading to interesting property of the derived complexes. Such a strategy has been exploited to mimic nitrate reductase activity.^{13b} The generality of such a reaction is under investigation which would be published later.

Acknowledgment. A.M. and K.P. gratefully acknowledge predoctoral fellowships from the CSIR, New Delhi, and S.S. thanks DST, New Delhi, for funding the project.

Supporting Information Available: Electronic spectra for the complexes **1–4**, **1a–4a**, and **5a**, UV–vis spectrophotometric monitoring for the conversion of **1** and **1a** to respective tris complexes; cyclic voltammogram, differential pulse polarograph, and crystallographic data in tabular form for complex **5a**. X-ray crystallographic files in CIF format for all the nine complexes (**1–4** and **1a–5a**). This material is available free of charge via the Internet at <http://pubs.acs.org>.

IC7006777